spotDNN: Provisioning Spot Instances for Predictable Distributed DNN Training in the Cloud

***Abstract*—Distributed Deep Neural Network (DDNN) training on cloud spot instances is increasingly compelling as it can significantly save the user budget. To handle unexpected instance revocations, provisioning a *heterogeneous* cluster using the asynchronous parallel mechanism becomes the *dominant* method for DDNN training with spot instances. However, blindly provisioning a cluster of spot instances can easily result in *unpredictable* DDNN training performance, mainly because bottlenecks occur on the parameter server network bandwidth and PCIe bandwidth resources, as well as the inadequate cluster heterogeneity. To address the challenges above, we propose *spotDNN*, a heterogeneity-aware spot instance provisioning framework that provides predictable performance for DDNN training in the cloud. By explicitly considering the contention for bottleneck resources, we first build an *analytical* performance model of DDNN training in heterogeneous clusters. It leverages the *weighted average batch size* and *convergence coefficient* to quantify the DDNN training loss in heterogeneous clusters. Through a lightweight workload profiling, we further design a *cost-efficient* instance provisioning strategy which incorporates the *bounds calculation* and *sliding window* techniques to effectively guarantee the training performance service level objectives (SLOs). We have implemented a prototype of *spotDNN* and conducted extensive experiments on Amazon EC2. Experiment results show that *spotDNN* can deliver predictable DDNN training performance while reducing the monetary cost by up to 68.1% compared to the existing solutions, yet with acceptable runtime overhead.**

***Index Terms*—distributed DNN training, predictable performance, spot instance provisioning, heterogeneous clusters**

I. Introduction

As Deep Neural Network (DNN) models get deeper and the training datasets get larger, distributed DNN (DDNN) training in the cloud becomes increasingly compelling [1]. To improve resource utilization [2], cloud providers offer users with idle computing resources at a 60%-80% discount, such as AWS spot instances, Google Spot VMs, and Azure Spot VMs [3]. Though at highly reduced prices, deploying DDNN training workloads on spot resources can suffer from severe performance degradation [4], which is mainly caused by unexpected instance revocations [5] and insufficient spot capacity due to user quotas [6]. To alleviate such performance degradation for DDNN training, provisioning a *heterogeneous* cluster of spot instances using the asynchronous parallel (ASP) mechanism [7] is becoming the *first choice* for cloud users.

However, finding the cost-efficient provisioning plan of heterogeneous clusters (*i.e.,* identifying the type and the number of spot instances) still remains challenging, even for sophisticated cloud users. They often rely on their own experience and intuition to provision spot instances for DDNN training [8]. Unfortunately, blindly provisioning heterogeneous instances

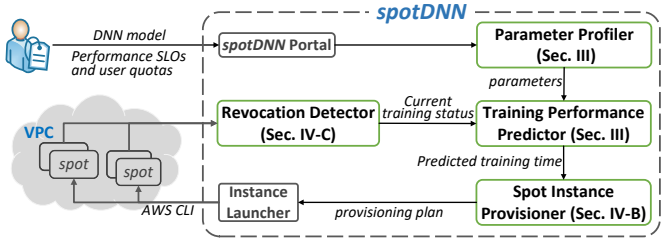

Fig. 1: Overview of *spotDNN*.

can result in *unpredictable* DDNN training performance due to the following two facts. *First,* the network bandwidth of the parameter server (PS) [9] and the limited PCIe bandwidth inside the instance can easily become bottleneck resources. As evidenced by our motivation experiment in Sec. II-B, the training time of VGG-19 can be prolonged by up to 65.7% as more spot instances are provisioned. *Second,* the inadequate cluster heterogeneity can impact the convergence rate of DDNN training due to the gradient staleness. Another motivation experiment in Sec. II-B shows that the convergence rate of ResNet-50 can vary by up to 39.8% as tuning the configuration of heterogeneous clusters. Accordingly, how to adequately provision spot instances to alleviate such unpredictable performance becomes the main *obstacle* to training DNN models cost-efficiently in the cloud.

To tackle such performance issues above, many efforts have been devoted to scheduling training jobs (*e.g.,* Gavel [10]), tuning the batch size (*e.g.,* LB-BSP [11]), migrating tasks with spot price prediction (*e.g.,* FarSpot [12]), and online batching (*e.g.,* DOLL [13]) in *homogeneous* DDNN training clusters. However, relatively little attention has been paid to adequately provision spot instances and guaranteeing the DDNN training performance in *heterogeneous* clusters. There have recently been works (*e.g.,* CM-DARE [8]) on modeling the training performance of heterogeneous clusters. Nevertheless, they imprecisely predict the training time due to neglecting the performance degradation caused by bottleneck resources. Though a more recent work (*i.e.,* Srifty [14]) leverages regression models and exhaustive search to identify the optimal instance provisioning plan in a heterogeneous cluster, it is hard to be applied in practice due to the heavy algorithm computation overhead. Moreover, characterizing the DDNN training loss in heterogeneous clusters has surprisingly been received little attention. As a result, scant research has been devoted to providing predictable DDNN training performance (*i.e.,* time and loss) by adequately provisioning a heterogeneous cluster of spot instances in a lightweight manner.

In this paper, we present *spotDNN* in Fig. 1, a heterogeneity-aware spot instance provisioning framework that guarantees DDNN training performance service level objectives (SLOs) in terms of objective training time and loss, while saving the training budget. By leveraging the parameters obtained through a lightweight workload profiling by the *parameter profiler*, we *first* devise an analytical performance model of DDNN training workloads in a heterogeneous cluster. The *training performance predictor* in *spotDNN* explicitly considers the performance degradation caused by bottleneck resources including the PS network bandwidth and limited PCIe bandwidth. It also leverages the *weighted average batch size* and the *convergence coefficient* to quantify the training loss in a heterogeneous cluster. *Second,* we design a cost-efficient instance provisioning strategy in *spot instance provisioner* to guarantee the training performance SLOs and minimize the training budget. It utilizes *bounds calculation* and *sliding window* to significantly reduce the algorithm computation overhead. By periodically checking the status of DDNN training and spot instances in the *revocation detector*, *spotDNN* is able to consider the performance impact of unexpected instance revocations, and it provisions takeover spot instances to guarantee the performance SLOs.

Finally, we implement a prototype[1] of *spotDNN* on AWS EC2 [6] and conduct extensive prototype experiments using four representative DNN models and seven types of spot instances. Experimental results demonstrate that *spotDNN* can deliver predictable performance for DDNN training while saving the user budget by up to 68.1% compared to the existing solutions, yet with a speedup of $10\times$ in computation overhead compared to the cutting-edge solution (*i.e.,* Srifty [14]).

The rest of the paper is organized as follows. Sec. II conducts an empirical study to analyze the key factors that affect DDNN training performance in heterogeneous clusters, which motivates the design of our analytical performance model of DDNN training workloads in Sec. III. Sec. IV presents the design and implementation of our *spotDNN* instance provisioning strategy. Sec. V evaluates the effectiveness and runtime overhead of *spotDNN*. Sec. VI discusses related work and Sec.VII concludes this paper.

II. Background and Motivation

In this section, we first seek to explore the key factors that impact the DDNN training performance in a heterogeneous cluster. We then present a motivation example to show how to provision heterogeneous spot instances to save the user budget while guaranteeing the training performance SLOs.

A. DDNN Training with Cloud Spot Instances

Though DDNN training with spot instances can significantly save the user budget, it is challenging because spot instances can be revoked at any time and the number of spot requests has a stringent limit (*i.e.,* user quota) [6]. To cope with such challenges above, we simply adopt a *heterogeneous* cluster of spot instances for DDNN training due to the following two facts. *First,* provisioning spot instances with one type is unlikely to meet workload performance requirements due to the user quotas. *Second,* heterogeneous instances can take over the training tasks of revoked instances as different instance types are commonly not revoked at the same time [5]. To efficiently train DNN models on heterogeneous spot instances, we focus on the ASP [15] mechanism under the PS architecture [9]. We have the following three benefits. *First,* ASP allows each worker[2] to communicate with the PS individually, and thus it breaks the synchronization barrier in the heterogeneous environment. *Second,* the training process will not be interrupted in ASP even when most of the workers are revoked [8]. *Third,* the newly-launched *takeover* instances can pull the latest model parameters directly from the PS, so as to reduce the recovery time of instance revocations.

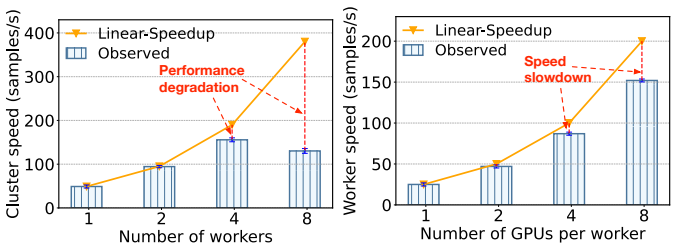

(a) (b)

Fig. 2: Training speed of VGG-19 on ImageNet obtained by (a) an n-worker cluster consisting of $\frac{n}{2}$ g3.4xlarge instances and $\frac{n}{2}$ g4dn.4xlarge instances, and (b) a G4dn instance with various number of GPUs.

B. Characterizing DDNN Training Performance in Heterogeneous Clusters

To explore the key factors of DDNN training performance in a heterogeneous cluster, we conduct motivation experiments on EC2 spot instances [6], by deploying P3, P2, G4dn, and G3 GPU instance types as workers and an m5.xlarge on-demand instance as the PS. We run three representative DDNN training workloads including ResNet-50 and ResNet-110 [16] on the CIFAR-100 [17] dataset, as well as VGG-19 [18] on a portion of the ImageNet [19] dataset. We illustrate the observed experiment results with error bars of standard deviation by repeating experiments 3 times.

Training Speed. To accelerate DDNN training, we simply set the batch size to fully utilize the GPU resource for each GPU type [11]. As shown in Fig. 2(a), the observed cluster speed first increases and then surprisingly decreases by up to 65.7% as the number of workers increases from 2 to 8 compared with the linear speedup curve. This is because the PS network bandwidth can easily become a *bottleneck resource* as the number of workers increases. To validate our analysis above, we record the PS network throughput over time, and the results show that the PS network bandwidth becomes saturated (*i.e.,* reaching up to 1.2 GBps) as the number of workers grows to around 8. Such an observation confirms our analysis of

[1]https://github.com/spotDNN/spotDNN

[2]We use *workers* and *instances* interchangeably in this paper.

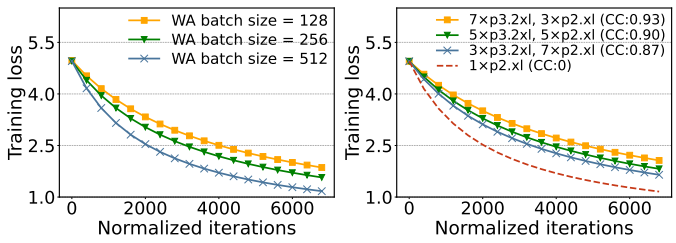

Fig. 3: Training loss of ResNet-50 on CIFAR-100 achieved by (a) various WA batch sizes on a heterogeneous cluster consisting of 6 workers (*i.e.,* 3× g3.4xl, 3× g4dn.4xl), and (b) various CCs on a heterogeneous cluster consisting of 10 workers with the WA batch size set as 256.

PS network bandwidth as a bottleneck resource even when training with the ASP mechanism in a heterogeneous cluster.

Moreover, the limited PCIe bandwidth within a worker is another key factor that affects the training speed. As shown in Fig. 2(b), the worker training speed slows down by up to 25.6% compared to the linear speedup curve, as the number of GPUs inside a worker varies from 2 to 8. This is because multiple GPUs in a worker contend for the limited PCIe bandwidth resource, prolonging the gradient aggregation time (linearly) with the number of GPUs. Accordingly, the PCIe bandwidth contention can cause a moderate speed slowdown, resulting in a *non-linear* acceleration of the training speed on a multiple-GPU instance.

Training Loss. To characterize DDNN training in heterogeneous clusters, we use a *weighted average (WA) batch size* to denote the average data size trained in an iteration. It can be defined as the amount of trained data samples per unit time divided by iterations trained per unit time. Deriving from Eq. (4) in Sec. III, the *weight* can be considered as the reciprocal of the worker iteration time. Accordingly, we define a *normalized iteration* as training a WA batch of data samples in a heterogeneous cluster. In particular, the WA batch size in a homogeneous cluster (*i.e.,* a special case of a heterogeneous cluster) is actually reduced to the batch size of a worker. As shown in Fig. 3(a), the DDNN training loss converges faster as the WA batch size increases. This is because a larger WA batch size generates a more accurate training gradient, achieving the objective training loss value with fewer iterations [20]. Accordingly, we can leverage the *WA batch size* to quantify the DDNN training loss in heterogeneous clusters.

Interestingly, we find that the cluster heterogeneity can impact the training loss by varying the numbers of p3.2xlarge and p2.xlarge instances in a 10-worker heterogeneous cluster, as illustrated in Fig. 3(b). Since workers can miss more fresh parameter updates in the ASP mechanism as the cluster scale increases [21], the *local training* with a single worker achieves the optimal loss convergence rate. To characterize the performance impact of cluster heterogeneity, we define a *convergence coefficient (CC)* as the *Euclidean distance* between the *parameter update vector* $W = [w^1, w^2, \ldots, w^{|\mathcal{N}|}]$ in a heterogeneous cluster $\mathcal{N}$ and the local training $W_{local} = [1, 0, \ldots, 0]$. In particular, we calculate the percentage of parameter updates w^i over the training process for each worker $i \in \mathcal{N}$, which denotes the *convergence contribution* of the worker to the model training. Accordingly, a smaller CC indicates a more *localized* model training where the training process is mainly distributed among fewer workers, thereby speeding up the convergence of training loss.

TABLE I: Comparison of the training time, monetary cost, and computation overhead of ResNet-110 with different instance provisioning strategies.

Strategies	Provisioning plans	Time (secs)	Cost / Overhead	
			Money ($)	Comp (secs)
On-demand	5×g3.8xl, 3×g3.16xl	2,549.02	17.75	0.02
CM-DARE$^+$	4×g3.8xl, 3×g3.16xl	2,710.85	5.16	0.02
Srifty$^+$	2×g4dn.4xl, 5×g3.8xl, 2×g3.16xl	2,597.34	4.97	0.21
spotDNN	5×g3.8xl, 3×g3.16xl	**2,549.02**	**5.33**	**0.02**

C. A Motivation Example

Blindly configuring heterogeneous clusters can either *under-provision* or *over-provision* instance resources, which can adversely affect the training performance. In response, we design *spotDNN* in Sec. IV to identify a cost-effective instance provisioning plan with predictable DNN training performance. We conduct a motivation experiment on ResNet-110 to illustrate its effectiveness. Specifically, we adopt g4dn.4xlarge, g3.8xlarge, g3.16xlarge, and p2.8xlarge instances each with a user quota of 5. The objective training loss is set as 0.8 and the objective training time is set as 2,600 seconds.

As shown in Table I, the CM-DARE$^+$ strategy, which combines the performance model of CM-DARE [8] with the *spotDNN* instance provisioning plan, produces a provisioning plan that exceeds the training objective time by 110.85 seconds. This is because CM-DARE$^+$ neglects the bottlenecks on PS network and PCIe bandwidth resources during the training process. It then overestimates the training performance and under-provisions spot instances. Furthermore, the Srifty$^+$ strategy, which combines the performance model of *spotDNN* and instance provisioning strategy (*i.e., exhaustive search* with a high complexity) of Srifty [14], configures 9 workers with the lowest budget but 10 times more computation overhead (*i.e.,* 0.21 seconds) than *spotDNN*. In contrast, *spotDNN* meets the training performance SLOs and saves the monetary cost by up to 69.9% compared to the cluster provisioned with on-demand instances (*i.e.,* the On-demand strategy with *spotDNN* instance provisioning plan).

Summary. *First,* the PS network bandwidth and the PCIe bandwidth can easily become bottleneck resources for DDNN training even in a heterogeneous cluster with the ASP mechanism. *Second,* the DDNN training loss essentially depends on the WA batch size, the CC, and the number of workers in a heterogeneous cluster. *Finally,* judiciously provisioning spot instances can significantly save monetary cost while guaranteeing performance SLOs for DDNN training workloads.

III. Modeling DDNN Training Performance in Heterogeneous Clusters

In this section, we first model the training loss using the WA batch size and the configuration of heterogeneous clusters

TABLE II: Key notations in our analytical performance model in heterogeneous clusters.

Notation	Definition
$\mathcal{N}$	Set of provisioned heterogeneous workers
j	Number of normalized iterations for a DNN model
T^i	Iteration time of a worker i
T_{exp}	Expected iteration time of a heterogeneous cluster
b_w	WA batch size of a heterogeneous cluster
v	Training speed of a heterogeneous cluster
R	CC of a heterogeneous cluster
T^i_{comm}	Communication time in each iteration of a worker i
S_{parm}	Parameter size of a DNN model
g^i	Number of GPUs in a worker i
B^i_{wk}	Available network bandwidth between a worker i and PS
B_{pcie}	Available PCIe bandwidth in a worker
B_{ps}	Available bandwidth of a PS node

(*i.e.,* the CC and the number of workers). We then predict the DDNN training time by explicitly considering the PS network and PCIe bandwidth resource bottlenecks. The notations in our performance model are summarized in Table II.

In general, the iteration time of DDNN training with the ASP mechanism can be different for heterogeneous workers. As elaborated in Sec. II, we characterize the DDNN training process in a heterogeneous cluster with j *normalized iterations*, and each iteration requires an *expected* iteration time T_{exp}. Therefore, we formulate the DDNN training time T as

$$T = j \cdot T_{exp}, \tag{1}$$

where T_{exp} is considered as the *expectation* of the iteration time of heterogeneous workers. Accordingly, T_{exp} can be formulated as the reciprocal of the number of iterations per unit time in a heterogeneous cluster, which is given by

$$T_{exp} = \frac{1}{\sum_{i\in\mathcal{N}} \frac{1}{T^i}}, \tag{2}$$

where $\mathcal{N}$ is the set of provisioned workers, and $\frac{1}{T^i}$ denotes the number of iterations per unit time on a worker i.

Modeling DDNN Training Loss. As discussed in Sec. II-B, the DDNN training loss converges faster as the WA batch size b_w gets larger and the CC R gets smaller. The convergence rate slows down as more workers are provisioned. Moreover, the DDNN training loss is inversely proportional to the normalized iterations j and converges at a rate of $\mathcal{O}(\frac{1}{j})$ [22]. Accordingly, we model the training loss in a heterogeneous cluster as

$$f_{loss}\left(b_w, R, \mathcal{N}, j\right) = \frac{\left(\gamma_2 \cdot b_w + \gamma_3\right)\sqrt{\left(R+\gamma_4\right)|\mathcal{N}|}}{j+\gamma_1} + \gamma_5, \tag{3}$$

where $\gamma_1, \cdots, \gamma_5$ are the model coefficients. In general, $\gamma_2 < 0$.

In a heterogeneous cluster, b_w is calculated as the ratio of trained data samples per unit time to iterations trained per unit time, as defined in Sec. II-B. In particular, the amount of data samples trained per unit time is considered as the cluster training speed (*i.e.,* v). The number of iterations trained per unit time can be identified as the *reciprocal* of the expected iteration time T_{exp}, according to Eq. (2). Accordingly, we formulate the WA batch size b_w as

$$b_w = \frac{v}{\frac{1}{T_{exp}}} = v \cdot T_{exp}. \tag{4}$$

As workers communicate with the PS without a synchronization barrier under the ASP mechanism, we calculate $v = \sum_{i\in\mathcal{N}} v^i = \sum_{i\in\mathcal{N}} \frac{b^i}{T^i}$, where v^i, b^i, and T^i denote the training speed, batch size, and iteration time of a worker i, respectively.

Moreover, the CC R is defined as the *Euclidean distance* between the parameter update vector of a heterogeneous cluster $W = \left[w^1, w^2, \ldots, w^{|\mathcal{N}|}\right]$ and the local training $W_b = [1, 0, \ldots, 0]$. We formulate it as

$$R = \sqrt{\left(w^1 - 1\right)^2 + \left(w^2 - 0\right)^2 + \ldots + \left(w^{|\mathcal{N}|} - 0\right)^2}, \tag{5}$$

where $w^i = \frac{v^i}{v}$ denotes the percentage of parameter updates for a worker i.

Modeling Iteration Time of a Worker. Each iteration of DDNN training is divided into two phases: gradient computation and parameter communication. They are processed sequentially under the ASP mechanism. Accordingly, we formulate the iteration time T^i of a worker i as

$$T^i = T^i_{comm} + T^i_{comp}, \tag{6}$$

where T^i_{comm} and T^i_{comp} denote the communication time and GPU computation time in an iteration of worker i, respectively. In particular, the GPU computation time T^i_{comp} is determined by the GPU type and batch size. Accordingly, we consider it as a constant value as long as the instance GPU types stay the same due to the same batch size for identical GPUs. We can calculate it as $T^i - T^i_{comm}$ by the workload profiling.

The communication phase consists of the gradient aggregation through PCIe and the parameter communication through the network. In general, the pushing and pulling of parameters can be considered as equal, and the size of model gradients is the same as that of model parameters (*i.e.,* S_{parm}). Accordingly, the communication time T^i_{comm} of a worker i can be calculated as

$$T^i_{comm} = \frac{2 \cdot S_{parm}}{B^i_{wk}} + \frac{2 \cdot g^i \cdot S_{parm}}{B_{pcie}}, \tag{7}$$

where B^i_{wk} denotes the available network bandwidth between a worker i and PS, and B_{pcie} denotes the available PCIe bandwidth in a worker with g^i GPUs.

As analyzed in Sec. II-B, B^i_{wk} is restricted by the PS network bandwidth B_{ps}, which becomes a resource bottleneck as more workers are provisioned. As shown in Fig. 4, the contention for PS network bandwidth only occurs during part of the communication phase because workers communicate with the PS at different times. Accordingly, we formulate the available network bandwidth B^i_{wk} of a worker i as

$$B^i_{wk} = \begin{cases} P \cdot \frac{B_{ps}}{|\mathcal{N}|} + (1-P) \cdot B_{req} & B_{req} > \frac{B_{ps}}{|\mathcal{N}|}, \\ B_{req} & B_{req} < \frac{B_{ps}}{|\mathcal{N}|}, \end{cases} \tag{8}$$

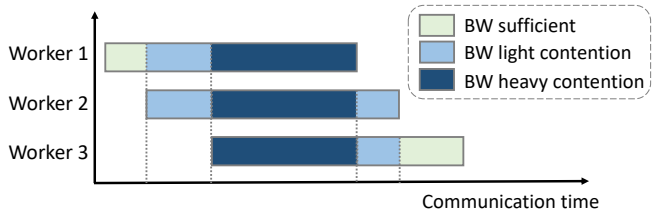

Fig. 4: Resource contention of PS network bandwidth (BW) over time as the communication between the worker and PS starts or ends.

where B_{req} denotes the network bandwidth requirement between a worker and PS when there is only one worker in the cluster. Besides, $P \in [0, 1]$ denotes the probability of PS network bandwidth bottleneck, which is positively correlated with the number of provisioned workers. We formulate it as

$$P = \min\left(\alpha_1 \cdot \sqrt{|\mathcal{N}|} + \beta_1,\ 1\right), \tag{9}$$

where α_1 and β_1 are model coefficients. In particular, $P = 1$ when the bandwidth competition reaches its peak.

Identifying Batch Sizes for Heterogeneous GPUs. To fully utilize the GPU resource, we assign a GPU of type k with its *largest* batch size b^k, which is usually a power of 2 and is limited by the GPU memory size. The relationship between b^k and the GPU memory usage mem^k can be formulated as

$$b^k = 2^{\lfloor \log_2(\alpha_2 \cdot mem^k + \beta_2) \rfloor}, \tag{10}$$

where α_2 and β_2 are model coefficients that can be obtained by workload profiling. We acquire b^k by setting mem^k as the GPU memory size. Accordingly, the batch size of a worker i with g^i GPUs of type k can be calculated as $b^i = g^i \cdot b^k$.

Obtaining Model Parameters. Based on the model above, we have 5 *workload-specific* parameters (*i.e.,* S_{parm}, B_{req}, α_i, β_i, γ_i) and 4 *instance-specific* parameters (*i.e.,* T^i_{comp}, g^i, B_{pcie}, B_{ps}). Specifically, the number of GPUs g^i in a worker i, the available PCIe bandwidth B_{pcie}, and the available bandwidth of the PS B_{ps} can be found in the instance configuration file of cloud providers. Then, we fit the model coefficients α_2 and β_2 by running the DNN model on a single worker with 30 iterations and recording the GPU memory usage under different batch sizes. Meanwhile, the model parameter size S_{parm} can be measured as the PS network data traffic divided by the number of iterations. The required network bandwidth B_{req} of workers can be obtained using the `nethogs` tool. To fast acquire the iteration time of different GPUs and the model coefficients (*i.e.,* α_1, β_1, and γ_i), we perform 3 epochs on three heterogeneous clusters with various numbers of workers (*i.e.,* 2, 4, 7) in parallel using the regression method [23]. With the obtained parameters above, the computation time T^i_{comp} of different GPUs can be calculated by Eqs. (6)-(7) accordingly.

IV. Guaranteeing DDNN Training Performance with Cloud Spot Instances

In this section, we first formulate the provisioning optimization problem of heterogeneous spot instances. We then design and implement our *spotDNN* instance provisioning strategy to provide predictable DDNN training performance.

A. Optimizing Spot Instance Provisioning

Given a set of available instance types $\mathcal{M}$, user quotas Lim (*i.e.,* the available number of instances for each type), and performance SLOs (*i.e.,* training time T_{obj} and loss value L_{obj}) for a DNN model, how can we adequately provision a set of spot instances $\mathcal{N}$ to guarantee the DDNN training performance while minimizing the monetary cost. The optimization problem can be formulated as

$$\min_{\mathcal{N}} \quad C = T \cdot \sum_{m \in \mathcal{M}} n_m \cdot p_m \tag{11}$$

$$\text{s.t.} \quad f_{loss}(b_w, R, \mathcal{N}, j) = L_{obj}, \tag{12}$$

$$T \le T_{obj}, \tag{13}$$

$$n_m \le Lim_m, \quad \forall m \in \mathcal{M}, n_m \in \mathcal{Z} \tag{14}$$

where n_m and p_m denote the provisioned number and the unit price of an instance type m, respectively. The output $\mathcal{N}$ is a list of the provisioned instances with a length of $\sum_{m \in \mathcal{M}} n_m$. The remaining objective training time T_{obj} requires re-calculation when instance revocations occur. Constraints (12) and (13) guarantee the training performance SLOs in terms of L_{obj} and T_{obj}. Constraint (14) denotes that the number of provisioned instances is below the user quota for each type m.

Problem Analysis. According to Eq. (11), the monetary cost C is actually impacted by the number of provisioned workers $|\mathcal{N}|$ and the training time T. By substituting Eqs. (2)-(10) into Constraint (13), we conclude that the constraint on the training time T is *non-linear*. As a result, our optimization problem in Eq. (11) turns out to be a *non-linear integer programming*, which is an NP-hard problem [24]. To solve such a problem, we adopt a heuristic algorithm for our instance provisioning problem.

To narrow down the solution search space, we design two optimization techniques. *First,* we analyze the lower bound n_{lower} and upper bound n_{upper} of the number of provisioned workers $|\mathcal{N}|$. As evidenced in Sec. II-B, the PS network bandwidth contention negatively impacts the training speed as more workers are provisioned. To avoid severe performance degradation, we let $P < 1$. According to Eq. (9), we calculate the upper bound n_{upper} as

$$n_{upper} = \left\lfloor \left(\frac{1 - \beta_1}{\alpha_1} \right)^2 \right\rfloor. \tag{15}$$

To meet the objective loss (*i.e.,* Constraint (12)), we can infer from Eq. (3) that the minimum number of normalized iterations is $\left(\frac{(\gamma_2 \cdot b_{\min} + \gamma_3)\sqrt{\gamma_4}}{L_{obj} - \gamma_5} - \gamma_1 \right)$, where $b_{\min} = \min_{i \in \mathcal{N}} b^i$ is the minimum batch size of all available instances. To meet the objective training time (*i.e.,* Constraint (13)), we can calculate the lower bound n_{lower} as

$$n_{lower} = \left\lceil \frac{b_{\min} \cdot \left(\frac{(\gamma_2 \cdot b_{\min} + \gamma_3)\sqrt{\gamma_4}}{L_{obj} - \gamma_5} - \gamma_1 \right)}{v_{\max} \cdot T_{obj}} \right\rceil, \tag{16}$$

where $v_{\max} = \max_{i \in \mathcal{N}} \frac{b^i}{T^i}$ is the maximum training speed of the available instances.

Algorithm 1: *spotDNN*: Heterogeneity-aware instance provisioning strategy for predictable performance of DDNN training with cloud spot instances.

Input: Performance SLOs (*i.e.,* training time T_{obj} and loss value L_{obj}) of a DNN model, a set of available instance types $\mathcal{M}$, user quotas Lim, and a list of existing instances E.
Output: Instance provisioning plan $\mathcal{N}$ and the monetary cost C.

1: Acquire *instance-specific* parameters (*i.e.,* T^k_{comp}, g^i, B_{pcie}, B_{ps}), and *workload-specific* parameters (*i.e.,* S_{parm}, B_{req}, α_i, β_i, γ_i) by lightweight workload profiling;
2: Calculate the batch size $b^k \leftarrow Eq.$ (10) and the computation time $T^k_{comp} \leftarrow Eq.$ (6) of GPU type k on a single-GPU instance;
3: **Initialize:** $C \leftarrow \infty$; $\mathcal{N} \leftarrow \emptyset$; Put all the available instances into the list I;
4: Calculate the upper bound $n_{upper} \leftarrow Eq.$ (15), the lower bound $n_{lower} \leftarrow Eq.$ (16), and the iteration time $T^i \leftarrow Eq.$ (6) of a worker i with the required network bandwidth B_{req};
5: Sort the available instances list I in descending order by T^i;
6: **for all** $n \in [n_{lower},\ n_{upper}]$ **do**
7: **for all** $idx \in [0,\ |I| - n]$ **do**
8: Acquire $\widehat{\mathcal{N}} \leftarrow E + I\,[idx,\ idx + n - 1]$ by *sequentially* selecting n instances from the idx-th instance in the available instances list I; `// sliding window`
9: Calculate the WA batch size $b_w \leftarrow Eq.$ (4), the CC $R \leftarrow Eq.$ (5), and the number of normalized iterations j to meet the objective loss value $f_{loss}(b_w, R, \widehat{\mathcal{N}}, j) \leftarrow L_{obj}$;
10: Calculate $\widehat{T} \leftarrow Eq.$ (1), $\widehat{C} \leftarrow Eq.$ (11);
11: **if** a revocation occurs **then**
12: $\widehat{T} \leftarrow \widehat{T} + T_{ohd}$; `// add revocation overhead`
13: **end if**
14: **if** $\widehat{T} \leq T_{obj}$ && $\widehat{C} < C$ **then**
15: Record the monetary cost $C \leftarrow \widehat{C}$ and the instance provisioning plan $\mathcal{N} \leftarrow \widehat{\mathcal{N}}$;
16: **end if**
17: **end for**
18: **end for**

Second, we aim to provision a set of spot instances with small differences in iteration time. We make the decision because such workers introduce a lower degree of gradient staleness [21], which makes the training loss converge more steadily. Accordingly, we store all the available instances in a list by sorting their iteration time in descending order. We then adopt a *sliding window* to select the *adjacent* instances with small differences in iteration time in the sorted list.

B. Design of spotDNN Instance Provisioning Strategy

Given a DNN model with the performance SLOs (*i.e.,* training time T_{obj} and loss value L_{obj}), a set of available instance types $\mathcal{M}$, the user quotas Lim, and a list of existing instances E, *spotDNN* first obtain the *instance-specific* parameters (*i.e.,* T^k_{comp}, g^i, B_{pcie}, B_{ps}) and the *workload-specific* parameters (*i.e.,* S_{parm}, B_{req}, α_i, β_i, γ_i) using a *lightweight* profiling method elaborated in Sec. III (line 1). It then calculates the batch size b^k and the computation time T^k_{comp} for a GPU type k (line 2). After initializing the monetary cost C, the provisioned plan $\mathcal{N}$, and the available instances list I, *spotDNN* calculates the upper bound n_{upper} and the lower bound n_{lower} of the number of provisioned workers (lines 3-4). By iterating each possible number n_i of provisioned workers, *spotDNN* considers the list of existing instances E and leverages a *sliding window* with the size n_i to select the possible provisioning plans $\widehat{\mathcal{N}}$ from the sorted instance list I (lines 5-8). *spotDNN* further calculates the number of normalized iterations j to meet the objective training loss value L_{obj} according to the WA batch size b_w and the CC R, and it obtains the estimated training time and monetary cost (lines 9-10). In particular, *spotDNN* adds an instance revocation overhead T_{ohd} (*e.g.,* less than 30 seconds) to the estimated training time $\widehat{T}$ when a revocation occurs (lines 11-13). Finally, *spotDNN* identifies a cost-efficient instance provisioning plan $\mathcal{N}$ that guarantees the objective time T_{obj} and minimizes the monetary cost C (lines 14-18).

Remark. The complexity of Alg. 1 is in the order of $\mathcal{O}(x \cdot y)$, where $x = n_{upper} - n_{lower} + 1$ denotes the possible search space of the number of provisioned workers $|\mathcal{N}|$, and $y = |I| - n_i + 1$ denotes the candidate provisioning plan under each possible number n_i. As a result, the computation overhead of *spotDNN* is well controlled and will be validated in Sec. V-D.

C. Implementation of our spotDNN Prototype

We implement a prototype of *spotDNN* on Amazon EC2 based on TensorFlow [25] v1.15.0 with over $1,000$ lines of Python and Linux Shell codes. To avoid network traffic across Availability Zones, we place all PS and worker instances within one Amazon Virtual Private Cloud (VPC). Our instance launcher uses the AWS CLI command to provision spot instances, particularly setting the `subnetID` according to the VPC information. To timely capture revocation events, our revocation detector periodically checks the instance status (*i.e.,* every 15 seconds) using the Amazon *instance metadata service*[3]. Once an instance revocation is detected, it first sends the current model training status (*i.e.,* the remaining instances and unfinished performance SLOs) to the training performance predictor. Then, *spotDNN* re-predicts the performance and launches *takeover* spot instances to guarantee the training performance. To achieve dynamic worker addition without interrupting the training process, *spotDNN* leverages *sparse mapping* [7] to store all the available IPv4 addresses in the VPC. It configures the newly added workers within the same VPC to enable efficient network communication. In particular, *spotDNN* can support other cloud platforms (*e.g.,* Google GCP, Microsoft Azure) by simply substituting AWS-related commands and metadata service APIs. The implementation details are described in our open-source codes on GitHub.

Discussion. *First, how does spotDNN deal with the prediction error of our performance model?* To mitigate the impact of SLO violations, *spotDNN* overpredicts the network contention in Eq. (9) by an empirical value (*e.g.,* $1 - 5\%$), which is the fluctuating range of network bandwidth B^i_{wk} based on our experiments in Sec. II-B. It can cause an underestimation

[3]https://docs.aws.amazon.com/AWSEC2/latest/WindowsGuide/ec2-instance-metadata.html

TABLE III: Configurations of EC2 instances used in our experiment.

Instance type	GPU devices	Max quota	Unit price ($)	
			spot[4]	on-demand
p3.2xlarge	1× V100	10	1.25	3.06
p2.8xlarge	8× K80	10	2.16	7.20
g4dn.12xlarge	4× T4	10	1.22	3.91
g4dn.4xlarge	1× T4	10	0.36	1.20
g3.16xlarge	4× M60	10	1.37	4.56
g3.8xlarge	2× M60	10	0.69	2.28
g3.4xlarge	1× M60	10	0.34	1.14

of the cluster training speed, making the training process faster than expected. As evidenced in Fig. 5, our bandwidth overprediction can basically offset the prediction error of the performance model.

Second, how to use spotDNN in multi-PS scenarios? spotDNN is applicable in multi-PS scenarios. Though adding more PS can alleviate the PS network bottleneck, the bottleneck still remains as it is intrinsic to the PS architecture. By simply replacing B_{ps} with the total network bandwidth that multi-PS provides, our performance model can readily be applied to multi-PS scenarios.

V. Performance Evaluation

In this section, we evaluate *spotDNN* by carrying out a set of prototype experiments on Amazon EC2 [6]. We seek to answer the following questions:

- **Accuracy:** Can our performance model in *spotDNN* predict the DDNN training performance (*i.e.,* time and loss) in heterogeneous clusters? (Sec. V-B)
- **Effectiveness:** Can our instance provisioning strategy in *spotDNN* provide predictable training performance while saving the monetary cost? (Sec. V-C)
- **Overhead:** How much runtime overhead of workload profiling and algorithm computation does *spotDNN* practically bring? (Sec. V-D)

A. Experimental Setup

Training Cluster Configurations. We deploy an m5.xlarge on-demand instance to serve as the PS. We provision heterogeneous workers with 7 representative instance types listed in Table III. To reduce the network traffic cost, we configure the provisioned instances within a VPC in the AWS us-east-1b region. In addition, the available bandwidth for the PS and the available PCIe bandwidth inside a worker is set as 1.2 GBps and 10 GBps, respectively.

Configurations of DNN Training Workloads. We select four representative DNN models as listed in Table. IV. Due to the budget limit, we only adopt CIFAR-100 [17] as the training dataset for VGG-19 [18], Inception-v3 [26], and ResNet-110 [16] models for image classification. We also choose an NLP DNN model (*i.e.,* EsperBERTo [27]) trained on the Esperanto portion of the OSCAR dataset[5].

[4]We list the spot price during the period of our experiments (Jan. 2023).
[5]https://oscar-corpus.com/

TABLE IV: Workload-specific parameters of representative DNN models.

Workload	ResNet-110	EsperBERTo	VGG-19	Inception-v3
Dataset	CIFAR-100	OSCAR	CIFAR-100	CIFAR-100
S_{parm} (MB)	11.54	336	574	98
B_{req} (MBps)	142	543	620	562

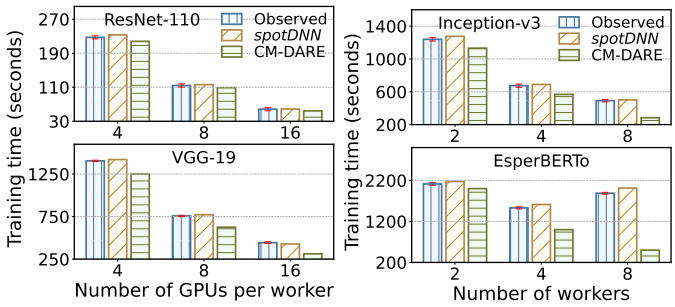

Fig. 5: Comparison of the observed and predicted training time with *spotDNN* and CM-DARE by using (a) a P2 instance by varying the number of GPUs per instance from 4 to 16, and (b) n-worker heterogeneous clusters consisting of $\frac{n}{2}$ g4dn.4xlarge and $\frac{n}{2}$ g3.16xlarge workers.

Baselines and Metrics. We compare *spotDNN* with the three strategies as discussed in Sec. II-C. In brief, CM-DARE$^+$ considers the cluster speed as the sum of ideal GPU training speeds [8]. Srifty$^+$ can be considered as the optimal solution based on the exhaustive search [14]. We focus on three key metrics including the DDNN training time, the monetary cost, and the computation overhead.

B. Validating Training Performance Model in spotDNN

Can *spotDNN* well predict the DDNN training time? We train the ResNet-110, VGG-19, Inception-v3, and EsperBERTo models for 10, 5, 6, and 1.5 epochs, respectively. As shown in Fig. 5(a), we observe that *spotDNN* can well predict the DDNN training time on a GPU instance, with a prediction error from 0.2% to 2.5%. In contrast, CM-DARE poorly predicts the DDNN training time as it overlooks the performance impact of PCIe bandwidth bottleneck during the gradient aggregation. The prediction error of the VGG-19 achieved by CM-DARE gets larger (*i.e.,* from 13.7% to 28.5%) as the number of GPUs on a worker increases from 4 to 16. This is because the PCIe bandwidth contention within a worker increases the gradient aggregation time, thereby causing a nonlinear speedup of the training speed.

Furthermore, Fig. 5(b) shows that *spotDNN* can accurately predict the DDNN training time in a heterogeneous cluster with a prediction error of 1.8% to 6.9% as the cluster scale varies from 2 to 8. However, CM-DARE fails to predict the training time with a prediction error reaching up to 73.5%. The rationale is that the contention of PS network bandwidth among workers gets severe as the number of provisioned workers and the parameter size increase, which is ignored by CM-DARE and thus leads to inaccurate training time prediction. As the number of workers increases from 4 to 8, the PS network bandwidth contention among workers dominates

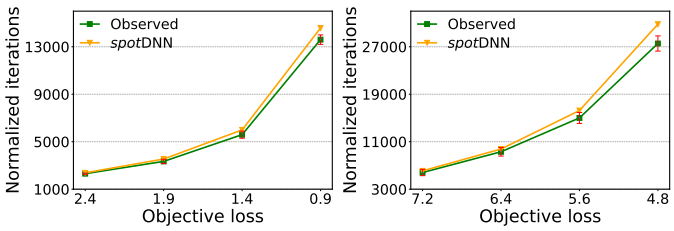

(a) ResNet-110 (b) EsperBERTo

Fig. 6: Comparison of the observed and predicted number of normalized iterations under different objective loss values with a heterogeneous cluster consisting of 4 g4dn.4xlarge and 4 g3.16xlarge workers.

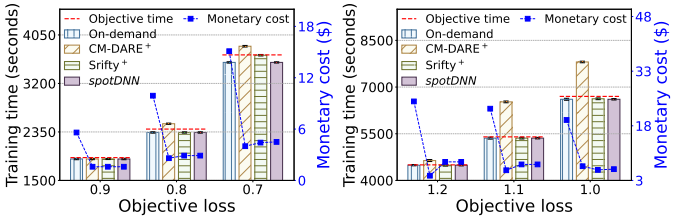

(a) ResNet-110 (b) Inception-v3

Fig. 7: Comparison of DDNN training time and monetary cost of various instance provisioning strategies under different performance SLOs.

the training process of EsperBERTo, thereby increasing the DDNN training time.

Can *spotDNN* well predict the DDNN training loss? We further evaluate the accuracy of our DDNN training loss model in an 8-worker heterogeneous cluster by setting the objective loss value as 2.4, 1.9, 1.4, 0.9 for ResNet-110 and 7.2, 6.4, 5.6, 4.8 for EsperBERTo, respectively. As shown in Fig. 6, we observe that *spotDNN* can basically predict the number of normalized iterations to converge to different objective loss values. Specifically, *spotDNN* achieves a prediction error of 4.8% – 11.7% for EsperBERTo, which is higher than that of ResNet-110 (*i.e.,* 3.1% – 7.1%). This is because large models (*i.e.,* EsperBERTo) consume more bandwidth resources to transfer gradients in the communication phase. It leads to severe contention of the PS network bandwidth and PCIe bandwidth, making the training performance fluctuate moderately (*i.e.,* up to 1,261 normalized iterations).

C. Effectiveness of spotDNN Instance Provisioning Strategy

Can *spotDNN* guarantee the DDNN training performance while minimizing the monetary cost? To examine the efficacy of our instance provision strategy, we set three different training performance SLOs listed in Table V for ResNet-110 and Inception-v3. As shown in Fig. 7, we observe that *spotDNN* can well meet the objective training time under different objective loss values, while saving the monetary cost by up to 68.1% compared with the three strategies. Specifically, CM-DARE+ can hardly provide predictable training performance for DNN models, because it neglects the bottlenecks on PS network and PCIe bandwidth resources. In contrast, both *spotDNN* and Srifty+ can guarantee training performance while reducing the budget. In most cases, *spotDNN* can obtain the optimal resource provisioning plans with Srifty+, as listed

TABLE V: Comparison of instance provisioning plans achieved by on-demand, CM-DARE+, Srifty+, and *spotDNN* for ResNet-110 and Inception-v3. The provisioning plan in the array is defined as [#p3.2xl, #g4dn.4xl, #g3.8xl, #g3.16xl, #p2.8xl].

	Workloads/ Strategies	**Performance SLOs** (loss value, training time)		
		(0.9, 1900)	(0.8, 2400)	(0.7, 3700)
ResNet-110	On-demand	[2, 0, 2, 0, 0]	[2, 0, 4, 0, 0]	[2, 1, 4, 0, 0]
	CM-DARE+	[2, 0, 2, 0, 0]	[2, 0, 3, 0, 0]	[2, 0, 3, 0, 0]
	Srifty+	[2, 0, 2, 0, 0]	[2, 0, 4, 0, 0]	[2, 1, 3, 0, 0]
	spotDNN	[2, 0, 2, 0, 0]	[2, 0, 4, 0, 0]	[2, 1, 4, 0, 0]
		(1.2, 4500)	(1.1, 5400)	(1.0, 6700)
Inception-v3	On-demand	[2, 0, 0, 3, 0]	[2, 0, 0, 2, 0]	[2, 0, 1, 0, 0]
	CM-DARE+	[2, 0, 0, 1, 0]	[0, 5, 2, 0, 0]	[0, 5, 2, 0, 0]
	Srifty+	[2, 0, 0, 3, 0]	[2, 0, 0, 2, 0]	[2, 0, 2, 0, 0]
	spotDNN	[2, 0, 0, 3, 0]	[2, 0, 0, 2, 0]	[2, 0, 1, 0, 0]

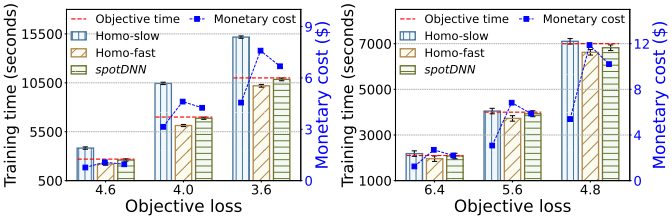

(a) VGG-19 (b) EsperBERTo

Fig. 8: Comparison of DDNN training time and monetary cost achieved by *spotDNN* and two homogeneous instance provisioning strategies.

in Table V. The rationale is that *spotDNN* simply uses a *sliding window* to capture the majority of near-optimal solutions, as discussed in Sec. IV-A. Furthermore, *spotDNN* can generate the instance provisioning plans much faster than Srifty+ by 84.6% (*i.e.,* 0.2 seconds *vs.* 1.3 seconds) when the user quota is set as 25. We will elaborate the computation overhead of *spotDNN* in a large cluster in Sec. V-D.

Can *spotDNN* outperform homogeneous instance provisioning strategies? To illustrate the training efficiency of heterogeneous clusters, we evaluate *spotDNN* against two homogeneous instance provisioning strategies (*i.e.,* Homo-slow, Homo-fast). Homo-slow provisions a cluster of instances with the slowest training speed, while Homo-fast provisions instances with the fastest training speed in the *spotDNN* provisioning plan. Both strategies provision the same number of workers as *spotDNN*. By setting three training performance SLOs listed in Table VI, we observe from Fig. 8 that *spotDNN* outperforms both Homo-slow and Homo-fast strategies. Specifically, Homo-slow violates the time constraint due to the inefficiency of slower instances and the longer training time required by the clusters with larger CCs. Though Homo-fast can guarantee the performance SLOs as *spotDNN*, its monetary cost increases by up to 18.5% due to the high unit price of instances. In contrast, *spotDNN* configures heterogeneous clusters with smaller CCs than homogeneous strategies. It ensures fast convergence even with several slower instances while saving the training budget.

TABLE VI: Comparison of instance provisioning plans and the corresponding CCs achieved by *spotDNN*, Homo-slow, and Homo-fast strategies for VGG-19 and EsperBERTo. The provisioning plan in the array is defined the same as Table V.

	Workloads/ Strategies	Performance SLOs (loss value, training time)		
		(4.6, 2700)	(4.0, 7000)	(3.6, 11000)
VGG-19	Homo-slow	[0, 2, 0, 0, 0] / 0.71	[0, 3, 0, 0, 0] / 0.82	[0, 3, 0, 0, 0] / 0.82
	Homo-fast	[2, 0, 0, 0, 0] / 0.71	[3, 0, 0, 0, 0] / 0.82	[3, 0, 0, 0, 0] / 0.82
	spotDNN	[1, 1, 0, 0, 0] / 0.51	[2, 1, 0, 0, 0] / 0.75	[2, 1, 0, 0, 0] / 0.75
		(6.4, 2100)	(5.6, 4000)	(4.8, 7000)
EsperBERTo	Homo-slow	[0, 0, 3, 0, 0] / 0.82	[0, 0, 4, 0, 0] / 0.87	[0, 0, 4, 0, 0] / 0.87
	Homo-fast	[0, 0, 0, 3, 0] / 0.82	[0, 0, 0, 4, 0] / 0.87	[0, 0, 0, 4, 0] / 0.87
	spotDNN	[0, 0, 1, 2, 0] / 0.59	[0, 0, 1, 3, 0] / 0.83	[0, 0, 1, 3, 0] / 0.83

Can *spotDNN* guarantee DDNN training performance even when revocations occur? As shown in Fig. 9, *spotDNN* starts the training of ResNet-110 by provisioning 3 g3.16xlarge and 5 g3.8xlarge instances. At the 29.8-th minute, the revocation detector in *spotDNN* captures the revocation signal, and it identifies 5 g3.8xlarge instances will be revoked. Leveraging the current training status (*i.e.,* remaining 3 g3.16xlarge instances, remaining training time as 810 seconds, and loss value as 0.9), the performance predictor further works with the instance provisioner in *spotDNN* to generate a new provisioning plan. Specifically, *spotDNN* launches 3 p3.2xlarge instances to *takeover* the unfinished model training work. In particular, the 3 newly added workers only spend 2.1 minutes joining the training process, which is slightly longer than the 2-minute notification [6] (*i.e.,* the 5 g3.8xlarge instances are revoked at the 31.4-th minute). Due to the fast failover mechanism of *spotDNN*, the performance degradation only lasts for 29.6 seconds (*i.e.,* from the 31.4-th to 31.9-th minute), as depicted in Fig. 9. *spotDNN* successfully achieves the training performance SLOs of ResNet-110 by completing the training process at the 41.9-th minute.

D. Runtime Overhead of spotDNN

We evaluate the runtime overhead of *spotDNN* in terms of the workload profiling overhead and the computation overhead of Alg. 1. Specifically, we launch a p2.xlarge EC2 instance to profile the *workload-specific* parameters (*i.e.,* S_{param}, B_{req}, α_2, β_2). By training the four DNN models for 30 iterations, the profiling time of ResNet-110 [16], Inception-v3 [26], VGG-19 [18], and EsperBERTo [27] models are merely 114, 75, 141, and 21.9 seconds, respectively. The remaining parameters (*i.e.,* α_1, β_1, γ_i) are profiled in parallel on 3 heterogeneous clusters with 2, 4, 7 workers. The profiling time of the four workloads is 0.6, 5.8, 12.8, and 11.7 minutes, respectively. Such job profiling overhead is negligible compared to the several hours required by a typical DDNN training workload.

To illustrate the computation overhead of *spotDNN*, we conduct another experiment by provisioning a ResNet-110 model using 70 available instances (*i.e.,* the maximum user quota) in Table III. *spotDNN* can achieve the optimal provisioning plan as Srifty$^+$ with a negligible computation overhead (*i.e.,* 0.3 seconds). In contrast, the computation overhead of Srifty$^+$ increases to $1,503.7$ seconds, due to the exhaustive search with the complexity in the order of $\mathcal{O}\left(\prod_{i\in\mathcal{M}} \mathrm{Lim}_i\right)$. Accordingly, *spotDNN* can be applicable to large-scale clusters and its runtime overhead is practically acceptable.

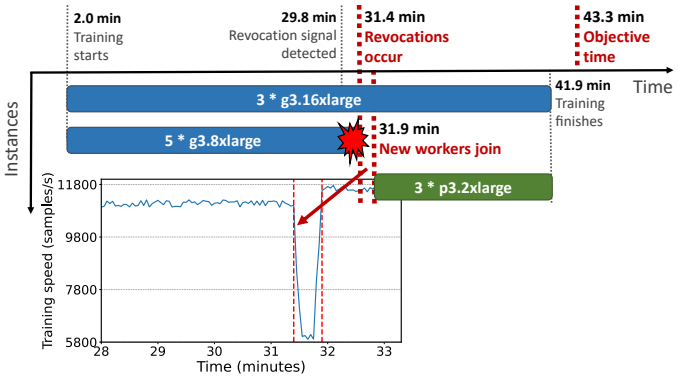

Fig. 9: Timeline of *spotDNN* dealing with multiple instance revocations, during the training process of ResNet-110 with an objective loss of 0.8 and an objective time of $2,600$ seconds.

VI. Related Work

Resource Provisioning of DDNN Training. To improve the DDNN training performance, Proteus [28] scales the cluster resources with on-demand and spot instances. FC^2 [29] aims to save the budget by considering the capacity and utilization of network bandwidth during resource provisioning. λDNN [30] and Cynthia [1] provision homogeneous workers with serverless functions and EC2 instances, respectively. However, we focus on the *heterogeneous* clusters while handling spot instance revocations without interruption. A more recent work Srifty [14] leverages the exhaustive search method to provision heterogeneous spot instances for DDNN training with the AllReduce architecture. In contrast, *spotDNN* designs a heuristic algorithm to dramatically reduce the computation overhead as evidenced in Sec. V-D. Also, *spotDNN* constructs an analytical performance model to predict training speed and loss, while Srifty relies on regression models which highly depend on the quality of training data and model features.

Performance Modeling of DDNN Training. Several works focus on modeling the training performance of *homogeneous* clusters, such as predicting the training time of DNN operations [31], simulating the interaction between the PS and workers [32], and predicting the training loss through online fitting [22]. CM-DARE [8] performs regression fitting on the training speed of heterogeneous clusters without considering the performance degradation caused by bottleneck resources. Jiang et al. [33] *qualitatively* analyze the impact of cluster heterogeneity on the DDNN training loss. Unlike prior works, *spotDNN* *quantitatively* models the training loss by introducing the *WA batch size* and *CC*. Moreover, it models the DDNN training time of *heterogeneous* clusters by explicitly considering the contention of PS network bandwidth and PCIe bandwidth with the ASP mechanism.

Fault Tolerance of Cloud Spot Instances. To enhance the spot instance availability, Spotlake [34] builds a random forest model based on historical spot price datasets. To handle spot

instance revocations, checkpointing is a straightforward and intuitive solution [3]. The checkpointing frequency can be optimized through online profiling of checkpointing overhead [4] or building a three-stage revocation probability model [35]. Bamboo [36] adds redundant computations to avoid data loss. Spotnik [37] designs an adaptive collective communication and synchronization mechanism for Ring-AllReduce. Orthogonal to these works above, we focus on the ASP mechanism under the PS architecture, which can *intrinsically* maintain the DDNN training process even when instance revocations occur. Moreover, we implement a revocation detector to provision takeover instances without interrupting the training process.

VII. Conclusion

This paper presents *spotDNN*, a heterogeneity-aware spot instance provisioning framework for achieving predictable DDNN training performance in the cloud. By explicitly considering the severe contention for the bottleneck bandwidth resources, *spotDNN* devises a lightweight analytical performance model for DDNN training in heterogeneous clusters. It leverages the WA batch size and CC to characterize the DDNN training loss in heterogeneous clusters. Such a performance model further guides the design of our cost-efficient spot instance provisioning strategy in *spotDNN*, which utilizes bounds calculation and sliding window to effectively identify the appropriate provisioning plan. Extensive prototype experiments on AWS EC2 demonstrate that *spotDNN* can deliver predictable DDNN training performance, while saving the monetary cost by up to 68.1% compared to existing solutions.

References

[1] H. Zheng, F. Xu, L. Chen, Z. Zhou, and F. Liu, "Cynthia: Cost-efficient cloud resource provisioning for predictable distributed deep neural network training," in *Proc. of ICPP*, Aug. 2019, pp. 1–11.

[2] S. M. Iqbal, H. Li, S. Bergsma, I. Beschastnikh, and A. J. Hu, "Cospot: a cooperative vm allocation framework for increased revenue from spot instances," in *Proc. of SOCC*, Nov. 2022, pp. 540–556.

[3] F. Xu, H. Zheng, H. Jiang, W. Shao, H. Liu, and Z. Zhou, "Cost-effective cloud server provisioning for predictable performance of big data analytics," *IEEE Transactions on Parallel and Distributed Systems*, vol. 30, no. 5, pp. 1036–1051, 2018.

[4] J. Mohan, A. Phanishayee, and V. Chidambaram, "CheckFreq: Frequent,Fine-Grained DNN Checkpointing," in *Proc. of USENIX FAST*, Feb. 2021, pp. 203–216.

[5] D. Narayanan, K. Santhanam, F. Kazhamiaka, A. Phanishayee, and M. Zaharia, "Analysis and exploitation of dynamic pricing in the public cloud for ml training," in *Proc. of VLDB Workshop*, Aug. 2020, pp. 1–8.

[6] Amazon. (2023, Feb.) Amazon EC2 Spot Instances. [Online]. Available: https://aws.amazon.com/cn/ec2/spot/

[7] S. Li, R. J. Walls, L. Xu, and T. Guo, "Speeding up deep learning with transient servers," in *Proc. of USENIX ICAC*, Jun. 2019, pp. 125–135.

[8] S. Li, R. J. Walls, and T. Guo, "Characterizing and Modeling Distributed Training with Transient Cloud GPU Servers," in *Proc. of IEEE ICDCS*, Nov. 2020, pp. 943–953.

[9] M. Li, D. G. Andersen, A. J. Smola, and K. Yu, "Communication efficient distributed machine learning with the parameter server," in *Proc. of NIPS*, Dec. 2014, pp. 1–9.

[10] D. Narayanan, K. Santhanam, F. Kazhamiaka, A. Phanishayee, and M. Zaharia, "Heterogeneity-Aware Cluster Scheduling Policies for Deep Learning Workloads," in *Proc. of USENIX OSDI*, Nov. 2020, pp. 481–498.

[11] C. Chen, Q. Weng, W. Wang, B. Li, and B. Li, "Accelerating Distributed Learning in Non-Dedicated Environments," *IEEE Transactions on Cloud Computing*, vol. preprint, pp. 1–17, 2021.

[12] A. C. Zhou, J. Lao, Z. Ke, Y. Wang, and R. Mao, "Farspot: Optimizing monetary cost for hpc applications in the cloud spot market," *IEEE Transactions on Parallel and Distributed Systems*, vol. 33, pp. 2955–2967, 2021.

[13] H. Jiang, X. Zhang, and C. Joe-Wong, "Doll: Distributed online learning using preemptible cloud instances," *ACM SIGMETRICS Performance Evaluation Review*, vol. 50, no. 2, pp. 21–23, 2022.

[14] L. Luo, P. West, P. Patel, A. Krishnamurthy, and L. Ceze, "SRIFTY: Swift and Thrifty Distributed Neural Network Training on the Cloud," in *Proc. of MLSys*, Aug. 2022, pp. 833–847.

[15] J. Dean, G. Corrado, R. Monga, K. Chen, M. Devin, M. Mao, M. Ranzato, A. Senior, P. Tucker, K. Yang *et al.*, "Large scale distributed deep networks," in *Proc. of NIPS*, Dec. 2012, pp. 1–9.

[16] K. He, X. Zhang, S. Ren, and J. Sun, "Deep residual learning for image recognition," in *Proc. of IEEE CVPR*, Jun. 2016, pp. 770–778.

[17] A. Krizhevsky, "Learning multiple layers of features from tiny images," University of Toronto, Toronto, Ontario, Technical Report, 2009.

[18] K. Simonyan and A. Zisserman, "Very deep convolutional networks for large-scale image recognition," in *Proc. of ICLR*, May 2015, pp. 1–14.

[19] A. Krizhevsky, I. Sutskever, and G. E. Hinton, "Imagenet classification with deep convolutional neural networks," *Communications of the ACM*, vol. 60, no. 6, pp. 84–90, 2017.

[20] X. Lian, Y. Huang, Y. Li, and J. Liu, "Asynchronous parallel stochastic gradient for nonconvex optimization," in *Proc. of NIPS*, Dec. 2015, pp. 2737–2745.

[21] J. Chen, X. Pan, R. Monga, S. Bengio, and R. Jozefowicz, "Revisiting distributed synchronous SGD," in *Proc. of ICLR Workshop*, May 2016, pp. 1–10.

[22] Y. eng, Y. Bao, Y. Chen, C. Wu, and C. Guo, "Optimus: an efficient dynamic resource scheduler for deep learning clusters," in *Proc. of EuroSys*, Apr. 2018, pp. 1–14.

[23] G. A. Seber and A. J. Lee, *Linear regression analysis*. John Wiley & Sons, 2012.

[24] S. Boyd, S. P. Boyd, and L. Vandenberghe, *Convex optimization*. Cambridge university press, 2004.

[25] M. Abadi, P. Barham, J. Chen, Z. Chen, A. Davis, J. Dean, M. Devin, S. Ghemawat, G. Irving, M. Isard *et al.*, "TensorFlow: a system for Large-Scale machine learning," in *Proc. of USENIX OSDI*, Aug. 2016, pp. 265–283.

[26] C. Szegedy, V. Vanhoucke, S. Ioffe, J. Shlens, and Z. Wojna, "Rethinking the inception architecture for computer vision," in *Proc. of IEEE CVPR*, Jun. 2016, pp. 2818–2826.

[27] J. Chaumond. (2020, Feb.) How to train a new language model from scratch using Transformers and Tokenizers. [Online]. Available: https://huggingface.co/blog/how-to-train

[28] A. Harlap, A. Tumanov, A. Chung, G. R. Ganger, and P. B. Gibbons, "Proteus: agile ml elasticity through tiered reliability in dynamic resource markets," in *Proc. of EuroSys*, Apr. 2017, pp. 589–604.

[29] N. B. D. Ta, "FC^2: cloud-based cluster provisioning for distributed machine learning," *Cluster Computing*, vol. 22, no. 4, pp. 1299–1315, 2019.

[30] F. Xu, Y. Qin, L. Chen, Z. Zhou, and F. Liu, "λDNN: Achieving Predictable Distributed DNN Training With Serverless Architectures," *IEEE Transactions on Computers*, vol. 71, no. 2, pp. 450–463, 2022.

[31] X. Y. Geoffrey, Y. Gao, P. Golikov, and G. Pekhimenko, "Habitat: A Runtime-Based Computational Performance Predictor for Deep Neural Network Training," in *Proc. of USENIX ATC*, Jul. 2021, pp. 503–521.

[32] Z. Li, W. Yan, M. Paolieri, and L. Golubchik, "Throughput prediction of asynchronous sgd in tensorflow," in *Proc. of ACM/SPEC ICPE*, Apr. 2020, pp. 76–87.

[33] J. Jiang, B. Cui, C. Zhang, and L. Yu, "Heterogeneity-aware distributed parameter servers," in *Proc. of ACM SIGMOD*, May 2017, pp. 463–478.

[34] S. Lee, J. Hwang, and K. Lee, "Spotlake: Diverse spot instance dataset archive service," in *Proc. of IISWC*, Nov. 2022, pp. 242–255.

[35] J. Kadupitige, V. Jadhao, and P. Sharma, "Modeling the temporally constrained preemptions of transient cloud vms," in *Proc. of ACM HPDC*, Jun. 2020, pp. 41–52.

[36] J. Thorpe, P. Zhao, J. Eyolfson, Y. Qiao, Z. Jia, M. Zhang, R. Netravali, and G. H. Xu, "Bamboo: Making preemptible instances resilient for affordable training of large dnns," *arXiv preprint arXiv:2204.12013*, 2022.

[37] M. Wagenlander, L. Mai, G. Li, and P. Pietzuch, "Spotnik: Designing distributed machine learning for transient cloud resources," in *Proc. of USENIX HotCloud*, Jul. 2020, pp. 1–8.